



Journal of Applied Sciences

ISSN 1812-5654

science
alert

ANSI*net*
an open access publisher
<http://ansinet.com>

Self Generated Fields Effects of Fast Electrons Beam on Plasma and Beam Characteristics

¹M. Mahdavi and ²S.F. Ghazizadeh

¹Department of Physics, Mazandaran University, P.O. Box 47415-416, Babolsar, Iran

²Department of Physics, Tehran Payam-e-Noor University, Tehran, Iran

Abstract: In this study, we investigate the self-generated the electric and magnetic fields effects of fast electrons beam on plasma and beam characteristics. The fields effect as; columbic transverse electric field, radial space charge potential, longitudinal plasma wakefield and transverse self magnetic field on beam propagational characteristics as; a collimated or focused and filamented beam and the plasma density perturbation are investigated. Also the hollowing effect due to self magnetic field which can generate an annular pattern in electrons beam is investigated.

Key words: Self generated fields, focusing, space-charge potential, wakefield, fast ignition, rigid beam, resistivity

INTRODUCTION

Fast electron propagation in plasma is always accompanied with self generated electric and magnetic fields which affect on plasma particles density and electron beam propagational characteristics. Self electric and magnetic fields make an electron beam collimated or focused and filamented (Hammer and Rostoker, 1970; Robinson and Sherlock, 2007). In some applications especially in Inertial Confinement Fusion (ICF) at fast ignition scheme, it is necessary to keep beam intensity and to control beam diverging or even increasing beam spot size intensity through focusing. The requirement for fast ignition are currently to be an electron beam energy at least 25 kJ, duration 10-20 ps, radius ~20 μm and electron kinetic energy of $E_b \approx 0.3-2$ MeV. The beam current typically is larger than 3×10^8 Amp and the maximum magnetic field associated with this huge current is tens of mega Gauss (Li and Petrasso, 2006). In sub-relativistic regime self electric field in vacuum is dominant over the magnetic field and the electron beam suffers naturally diverging but with increasing beam energy in relativistic regime (>1 MeV) up to ultra relativistic limit ($v \sim c$) magnetic force grows and is finally almost equal to electric force, and beam may be collimated (Humphries, 1990). In plasma, there is a different situation due to plasma response to beam presence, the magnetic field can be so large that beam may be focused. Beam hollowing in very high intensity and in time evolution may be generated and produces an annular pattern in which varies the beam spot size.

SELF GENERATED FIELDS

Self generated fields in vacuum: When an electron beam moves in vacuum, natural columbic repulsion expels the electrons off axes direction, the self electric field of the beam in vacuum is calculated as follows (Humphries, 1990):

$$E_r(r) = \frac{1}{2\pi\epsilon_0} \int_0^r 2\pi r' n(r') dr' \quad (1)$$

If the electron beam density is considered as:

$$n(r') = n_0 \exp\left(\frac{-r'^2}{2r_b^2}\right)$$

then the electron field will be obtained as:

$$E_r(r) = \frac{en_0 r_b^2}{\epsilon_0 r} \left[\exp\left(\frac{-r^2}{2r_b^2}\right) - 1 \right]$$

The self magnetic field is then obtained as:

$$B_r(r) = \left(\frac{\beta}{c}\right) E_r(r)$$

We can also determine the relation between two forces as; F_{rB} (magnetic) = $-\beta^2 F_{rE}$ (electric). Figure 1 shows the electric and magnetic forces as defocusing and focusing forces. The forces ratio, F_B/F_E approaches to unit with increasing beam

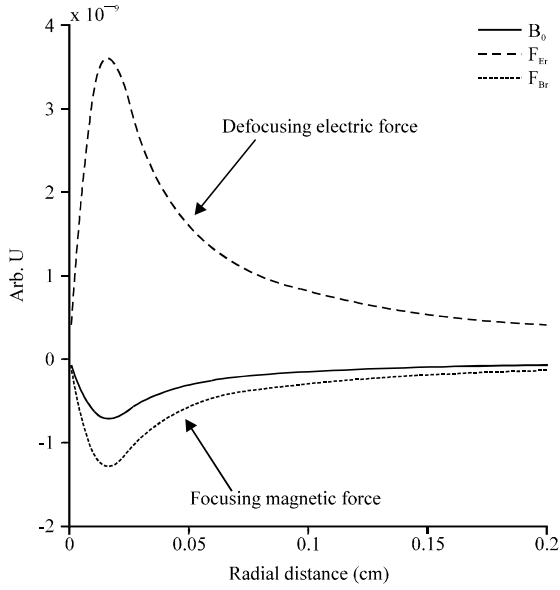


Fig. 1: Electric and magnetic forces act on electron with Gaussian beam profile in vacuum ($\beta = 0.6$)

velocity. In ultra relativistic limit ($v \sim c$) two forces balance and the electron beam moves collimately.

Space-charge potential and Wakefield due to beam arriving in plasma: Beam behavior in plasma is very different from vacuum. When an external charge arrives in plasma medium, the space charge potential is generated and plasma particles (mostly electrons) distribution are perturbed. Plasma particles are rearranged as the bulk of plasma keep and itself enclosed from this external charge. Plasma shields the charge and after some Debye length the potential in plasma returns back to its initial reference. If an electron beam arrives in plasma, the space-charge potential according to poisson's equation is generated. This potential affects on plasma and beam particles distribution. For an initial uniform plasma as; $n_e = n_i = n_0$, after beam arriving, the Poisson's equation is written as (Humphries, 1990):

$$\frac{1}{r} \frac{d}{dr} \left(r \frac{d\phi}{dr} \right) = \frac{e}{\epsilon_0} \left[n_{b0} f(r) - n_0 + n_0 \exp\left(\frac{e\phi}{kT_e}\right) \right] \quad (2)$$

where, $n_b = n_{b0} f(r)$ is beam profile. For the scale potential in terms of

$$kT_e, \phi = -\frac{e\phi}{kT_e}$$

and the length in terms of the Debye length, $R = r/\lambda_D$, the normalized form of Poisson's equation is rewritten as:

$$\frac{1}{R} \frac{d}{dR} \left(R \frac{d\phi}{dR} \right) = -n_{b0} f(R) + [1 - \exp(-\phi)] \quad (3)$$

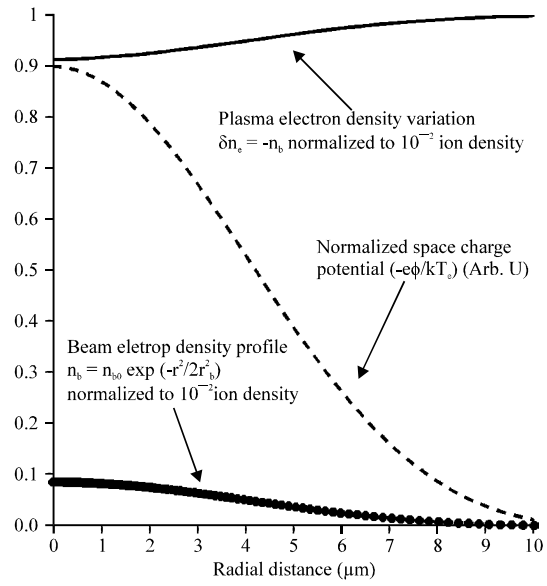


Fig. 2: Normalized space-charge potential variation (dashed line), plasma electron variation (solid line) and electron beam density variation (dotted line) due to Gaussian electron beam profile in unmagnetized uniform plasma versus normalized radial distance

Where:

$$N_{b0} = \frac{n_{b0}}{n_0}$$

and

$$n_{b0} = n_0 \exp\left(\frac{-r^2}{2r_b^2}\right)$$

therefore,

$$f(r) = \exp\left(\frac{-r^2}{2r_b^2}\right)$$

Now we can investigate the behavior of plasma and the beam particles after space-charge potential generation. In Fig. 2 we can see that the space-charge potential, after some Debye length, returns back to its initial reference (zero). Also Fig. 2 shows that the plasma electrons density is modulated as: $n_e(r) = n_{e0} \exp(-\phi)$ (Humphries, 1990; Esarey *et al.*, 1996). To keep charge neutralization in plasma after beam arriving, $\delta n_e = -n_b$ should be established. As we can see from Fig. 3, the electric field related to this plasma potential is directed off-axes, therefore, the force on the electrons of beam is directed on-axes and this field acts as a focusing force. If electron beam terminates in a time short compared to

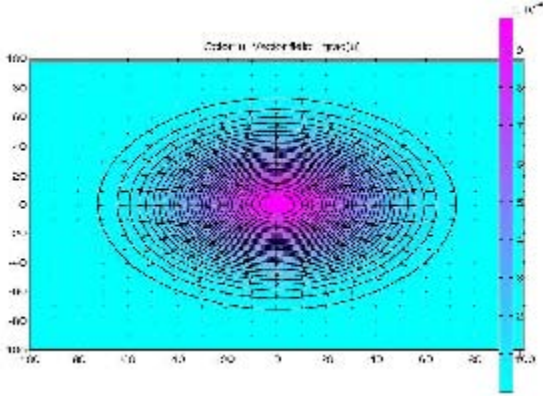


Fig. 3: Color map describes space-charge potential but vectors indicate the electric field related to this potential. This field is directed off-axes therefore acts as a focusing force on the electrons of beam

ω_{pe}^{-1} , in plasma Wakefield of the form, $\delta n = n_b \sin k_p (z-ct)$ will be generated (Esarey *et al.*, 1996). The axial electric field in linear regime is given by,

$$\frac{\partial E_z}{\partial z} = -4\pi e \delta n$$

so, we will get:

$$E_z = 4\pi e \left(\frac{n_b}{k_p} \right) \cos k_p (z-ct) \quad (4)$$

Figure 4 shows plasma Wakefield in two different beam densities with assuming a very long Gaussian beam:

$$n_{be} = n_{b0} \exp\left(\frac{-r^2}{2r_b^2}\right) \text{ with } \omega_b = \left(\frac{4\pi e^2 n_b}{m_e}\right)^{1/2}$$

arriving in plasma with

$$\omega_{pe} = \left(\frac{4\pi e^2 n_b}{m_e}\right)^{1/2}$$

When beam density approaches to plasma density, the Wakefield and plasma electron density perturbation approaches to a beat-like pattern (Fig. 5). Beam and plasma electrons accelerate and decelerate due to this Wakefield. For $n_{b0} = 10^{-2} n_0$ we obtain,

$$\left(\frac{\Delta n_e}{n_0}\right)_{\max} = 10^{-2}$$

and for the case $n_{b0} = 10^{-5} n_0$ we obtain:

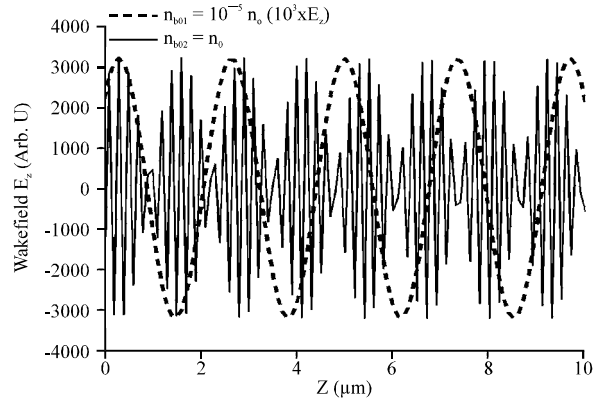


Fig. 4: Wakefield in two beam density values . Higher value of the beam density makes Wakefield beat like pattern

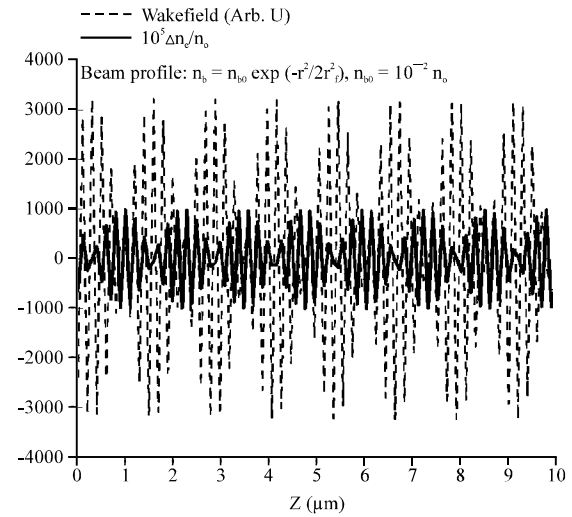


Fig. 5: Wakefield and relative variation of plasma electron density (shifted by 10^5 times) versus beam propagating direction due to a long Gaussian beam arriving in plasma. Wakefield with beat like pattern makes density variation as beat like as

$$\left(\frac{\Delta n_e}{n_0}\right)_{\max} = 10^{-5}$$

which the later is negligible (Fig. 6).

Time-independent self magnetic field of electron beam in plasma: The magnetic field of an electron beam can affect on its propagational characteristics and bends the particles trajectory. We consider an infinitely long cylindrical fast electron beam with the Lorentz factor γ_b , the radius r_b and the current of I_b propagating in plasma.

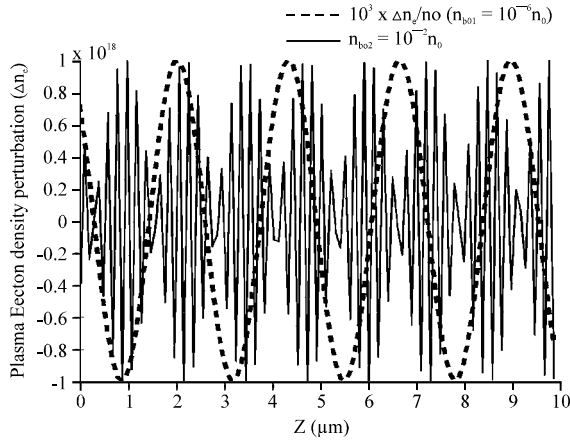


Fig. 6: Plasma electrons perturbation in two different beam density magnitudes. The oscillating pattern in beam density closer to plasma density is very different with the case of very lower

According to Ampere's law the time independent azimuthal magnetic field is given by:

$$B_\theta(r) = \frac{\mu_0 I_b F\left(\frac{r}{r_b}\right)}{2\pi r} \quad (5)$$

Where:

$$F\left(\frac{r}{r_b}\right)$$

is the fraction of current contained within a radius, r. The equation of motion for an electron beam in this field is given by Storm (2009):

$$\gamma_e m_e \frac{d^2 r}{dt^2} = e v_z B_\theta \quad (6)$$

recasting the Eq. 6 in terms of the dimensionless variables; $R = r/r_b$, $V_z = v_z/\beta c$, $\tau = t v_z/r_b$ and using $c^2 = 1/\epsilon_0 \mu_0$, the dimensionless equation of motion is:

$$\frac{d^2 R}{d\tau^2} = \frac{I_b}{[4\pi\epsilon_0 m_e c^3 \beta_b \gamma_b / e]} \frac{2V_z F(R)}{R} \quad (7)$$

The quantity in bracket has units of current and is defined as the Alfvén current I_A . After substituting the physical constants the Alfvén current for electrons can be expressed as $I_A \approx 17.1 \beta_b \gamma_b$ [KA].

If the electron beam current density is assumed uniform in radial direction then current fraction becomes:

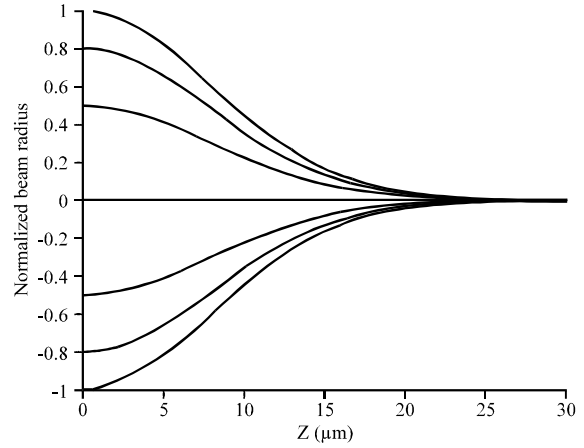


Fig. 7: Trajectory of electrons in self generated magnetic field of a uniform beam intensity profile in plasma medium ($I_b = 0.5 I_A$). Only considering magnetic field there is a certain focal point

$$F(R) = \frac{I}{I_b} = \frac{j\pi r^2}{j\pi r_b^2}$$

and the equation of motion becomes;

$$\frac{d^2 R}{dz^2} = \frac{I_b}{I_A} \left(\frac{2}{V_z}\right) R$$

The numerical solution of the above differential equation leads to a curve that is shown in Fig. 7. The particles of the beam in different radius are focused on a certain point, but actually coulombic repulsion makes impossible to reach a focused point. If we consider the current density profile as Gaussian;

$$j = j_0 \exp\left(\frac{-r^2}{2r_b^2}\right)$$

then we will have;

$$F(R) = \frac{R^2 \exp(-R^2/2)}{\exp(-1/2)}$$

Applying this profile with $I_b = 0.5 I_A$ (in inertial confinement fusion at fast ignition scheme $I_b \gg I_A$) in Eq. 7 leads to Fig. 8. As we can see, the particles in distant points experience larger magnetic field and therefore, have near focusing point than particles in closer points to beam axes. For $I_b \gg I_A$ the electrons trajectory so large bend in which the backward current is made and return current will partially neutralize the magnetic field due to

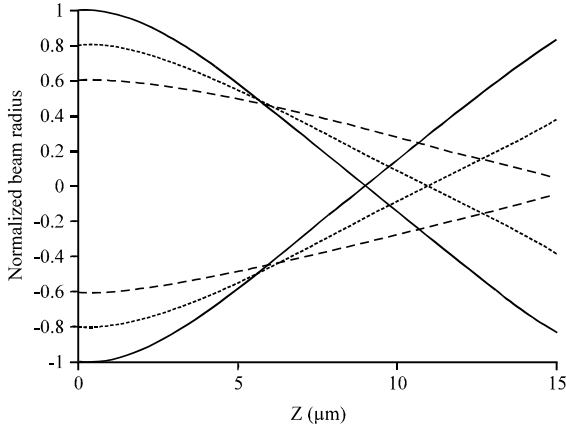


Fig. 8: Trajectory of electrons in self generated magnetic field of a non uniform beam intensity profile [$j = j_0 \exp(-r^2/2rb^2)$] in plasma medium (with $I_b = 0.5 I_A$). With considering only magnetic field we will have several focal points. Electrons in larger radius have closer focal points

the forward directed current. As a consequence, the fast-electron current and the corresponding magnetic field are reduced (Storm, 2009). Charged currents can be transported in vacuum only up to a maximum current, the so-called Alfvén current (Atzeni and Meyer-ter-Vehn, 2009). The physical reason for this limit is that currents larger than I_A generate a magnetic field large enough that the Larmor radius of the electrons becomes smaller than the beam radius. As a result the beam electrons are not further transported in beam direction. Although the Alfvén current limit does not apply globally to beam transport in plasma, it appears that the current in each filament cannot exceed I_A by a large factor (Atzeni and Meyer-ter-Vehn, 2009). We should notice that fast ignition requires fast electron beam with currents on the order of $I_b \approx 1000 I_A$. If electrical or magnetic neutrality is fractional the beam transportable current in plasma becomes more than without them. If f_E is the fractional electrical neutrality the limiting current becomes (Hammer and Rostoker, 1970):

$$I_{lim} \approx \frac{17.1 \gamma_b \beta_b^2}{\beta_b^2 + f_E - 1} [KA] \quad (8)$$

And if in addition f_M is the fractional degree of magnetic neutralization the limiting current becomes:

$$I_{lim} \approx \frac{17.1 \gamma_b \beta_b^2}{\beta_b^2 [1 - f_M] + f_E - 1} [KA] \quad (9)$$

Time -dependent self magnetic field of electron beam in plasma: The magnetic field at the previous section is

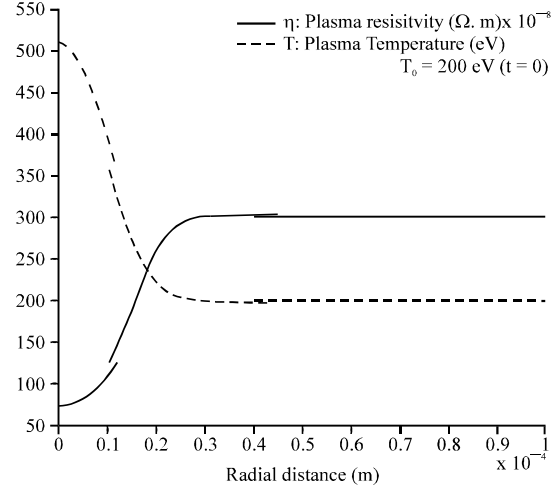


Fig. 9: Target resistivity variation due to beam arriving with Gaussian profile according to Spitzer limit for hot electrons (solid line) and temperature variation of target (dashed line) versus radial distance in $t = 50$ ps

assumed time independent and therefore Ampere's law has been applied. However, in more real situation for a non uniform beam, plasma resistivity is time-space dependent. Considering Faraday's law for the rate of magnetic field, we have (Robinson and Sherlock, 2007; Humphries, 1990; Davies *et al.*, 2006):

$$\frac{\partial B}{\partial t} = \eta \nabla \times j_b + \nabla \eta \times j_b \quad (10)$$

where, η and j_b are plasma resistivity and beam current density, respectively. Assuming rigid model beam (which assumes a static beam) and hot plasma with Spitzer limit for resistivity we have (Davies *et al.*, 2006):

$$\frac{\partial T_e}{\partial t} = \frac{\eta j_b^2}{c} \quad (11)$$

$$\eta = \eta_0 \frac{T^{-3/2}}{T_0} \quad (12)$$

The coupling of the above equations gives hand:

$$T = T_0 \left(1 + \frac{5}{2} \frac{\eta_0 j_b^2 \tau}{C T_0} \right)^{2/5} \quad (13)$$

where, C is a constant heat capacity and index zero indicates the initial situation. Finally we can determine the resistivity gradient as below:

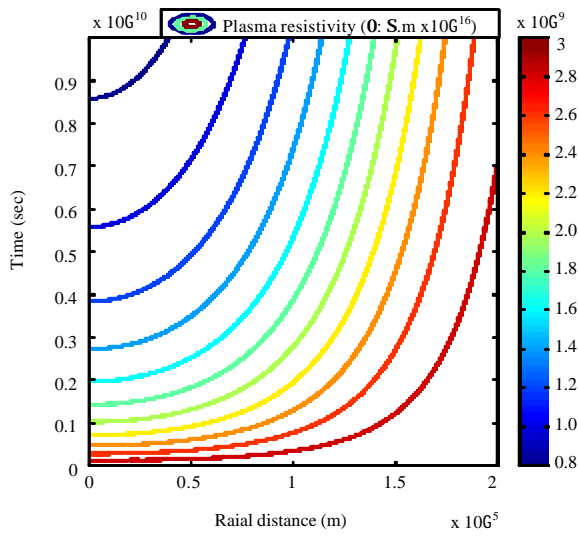


Fig. 10: Plasma resistivity contours $[\eta(r, t)]$. Each contour shows an equivalent resistivity in different time-space

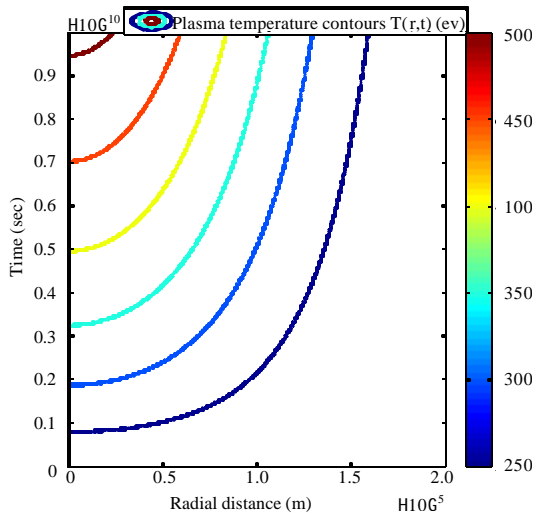


Fig. 11: Plasma temperature contours $[T(r, t)]$. Each contour shows an equivalent temperature in different time-space

$$\frac{\partial \eta}{\partial r} = \frac{\eta_0}{T_0} \frac{\partial T^{-3/2}}{\partial T} \frac{\partial T}{\partial r} \quad (14)$$

Figure 9 shows plasma temperature and resistivity at a same framework according to previous discussion. Figure 10 shows that resistivity decreases at a certain radius with time increasing and at a certain time is larger

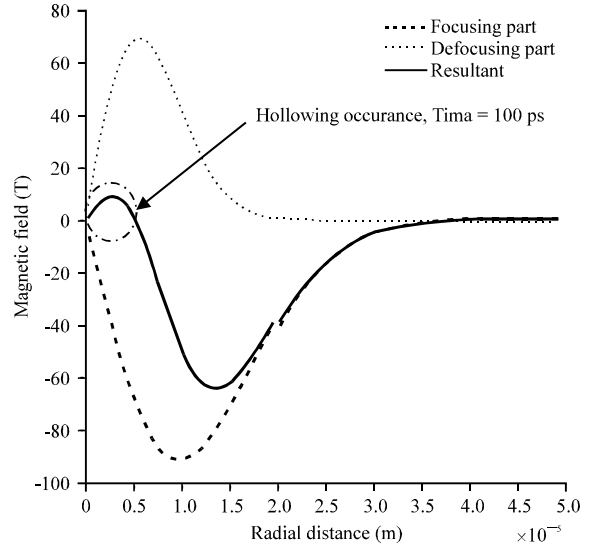


Fig. 12: Different self magnetic contributions and their resultant in $t = 100$ ps. Positive part is $\nabla \eta \times j_b$ which defocuses the beam and it is responsible to hollowing effect and negative part is $\eta \nabla \times j_b$ which focuses the beam

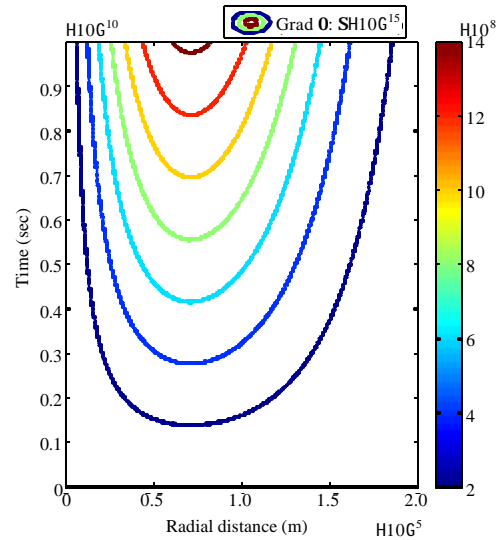


Fig. 13: Plasma resistivity gradient contours $[\nabla \eta(r, t)]$. Each contour shows an equivalent resistivity gradient in different time-space

in distant point of the beam axes. As we can see from Fig. 11, plasma temperature increases with time increasing and also at a certain time, temperature is maximum on the beam propagating axes. The self magnetic of the beam related to terms $\eta \nabla \times j_b$ and $\nabla \eta \times j_b$ produce different

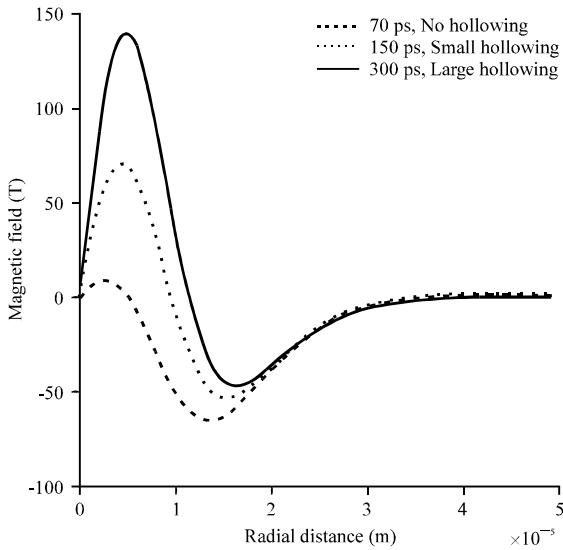


Fig. 14: Self magnetic field in different times versus radial distance. In high intensity but not very long time there is no hollowing (typical time duration of beam in fast ignition is 10-20 ps). Hollowing effect becomes significant with time increasing

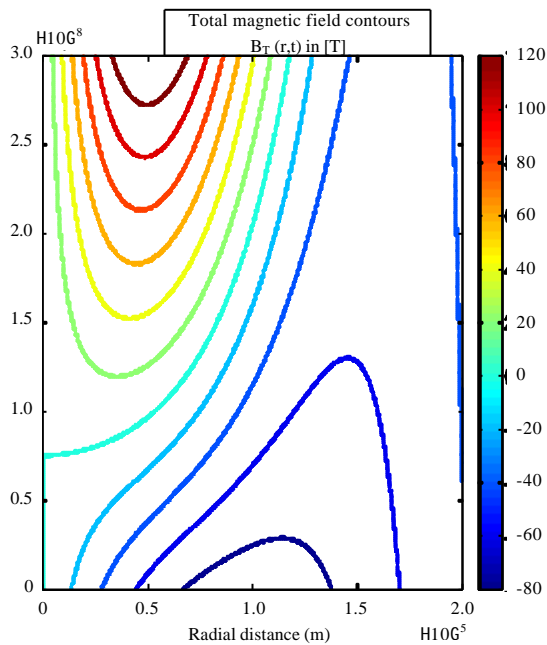


Fig. 15: Total self magnetic field contours $B_T(r, t)$. Each contour shows an equivalent magnetic field in different time-space

behavior for electrons in the beam (Solodov *et al.*, 2008). $\eta \nabla \times j_b$ Pushes the electrons to higher j_b and acts as a on-

axes force and focuses the beam but on the other hand $\nabla \eta \times j_b$ pushes the electrons to higher η and acts as a off-axes force and defocuses the beam (Robinson and Sherlock, 2007; Humphries, 1990; Storm, 2008; Kingham *et al.*, 2010). Figure 12 shows the effects of these two parts which have been calculated numerically in high current intensity $j_{b0} \geq 10^{15}$ (A/m²) and long pulse ($t \geq 100$ ps). The center part of the beam is purely defocused and hollowing effect occurs and the beam experiences an annular pattern (Davies *et al.*, 2006). The effects of two terms vary with time increasing. According to Fig. 13, $\nabla \eta$ increases with the increasing of time, therefore, the magnetic field related to $\nabla \eta \times j_b$ dominates than $\eta \nabla \times j_b$. As a result, if the pulse time to be long enough (in high intensity of beam) the hollowing occurrence becomes more possible (Fig. 14) (Norreys *et al.*, 2006). Figure 15 shows magnetic field contours $B_T(r, t)$ which Plus (minus) contours indicate defocusing (focusing) part.

CONCLUSIONS

Columbic repulsion naturally expels the electrons of a the beam to an off-axes direction but in plasma medium, space-charge potential acts as a focusing force. The plasma Wakefield, due to charge perturbation, generates an oscillating pattern field and therefore , the electrons accelerate and decelerate. The plasma Wakefield effect is negligible in the case of the low density. In the case of high intensity beam, the electric fields are less important than magnetic field. In time dependent situation, Fraday’s law determines the magnetic field. We showed that in high intensity and long pulse duration hollowing effect is obvious. In fast ignition, where duration is about 10-20 ps the hollowing effect in intensity 10^{15} (A/m²) is not significant but in time $t > 70$ ps in our model an annular pattern is produced.

REFERENCES

Atzeni, S. and J. Meyer-ter-Vehn, 2009. The Physics of Inertial Fusion: Beam Plasma Interaction, Hydrodynamics, Hot Dense Matter. Oxford University Press, Oxford, UK., ISBN-13: 9780199568017, Pages: 480.
 Davies, J.R., J.S. Green and P.A. Norreys, 2006. Electron beam hollowing in laser-solid interactions. Plasma Phys. Controlled Fusion, 48: 1181-1199.
 Esarey, E., P. Sprangle, J. Krall and A. Ting, 1996. Overview of plasma-based accelerator concepts. IEEE Trans. Plasma Sci., 24: 252-288.

- Hammer, D.A. and N. Rostoker, 1970. Propagation of high current relativistic electron beams. *Phys. Fluids*, 13: 1831-1850.
- Humphries, S., 1990. *Charged Particle Beams*. Wiley-Interscience Publication, New York, USA., ISBN-13: 9780471600145, Pages: 834.
- Kingham, R.J., M. Sherlock, C.P. Ridgers and R.G. Evans, 2010. Vlasov-Fokker-Planck simulations of fast-electron transport with hydrodynamic plasma response. *J. Phys. Conf. Ser.*, Vol. 244. 10.1088/1742-6596/244/2/022042
- Li, C.K. and R.D. Petrasso, 2006. Energy deposition of MeV electrons in compressed targets of fast-ignition inertial confinement fusion. *Phys. Plasma*, Vol. 13, No. 5. 10.1063/1.2178780
- Norreys, P.A., J.S. Green, J.R. Davies, M. Tatarakis and E.L. Clark *et al.*, 2006. Observation of annular electron beam transport in multi-TeraWatt laser-solid interactions. *Plasma Phys. Controlled Fusion*, 48: L11-L12.
- Robinson, A.P.L. and M. Sherlock, 2007. Magnetic collimation of fast electrons produced by ultraintense laser irradiation by structuring the target composition. *Phys. Plasma*, Vol. 14, No. 8. 10.1063/1.2768317
- Solodov, A.A., K.S. Anderson, R. Betti, V. Gotcheva and J. Myatt *et al.*, 2008. Simulations of electron transport and ignition for direct-drive fast-ignition targets. *Phys. Plasmas*, Vol. 15, No. 11. 10.1063/1.3000674
- Storm, M., 2008. High-current electron-transport studies using Coherent Transition Radiation (CTR). Proceedings of the 50th Annual Meeting of the American Physical Society Division of Plasma Physics, November 17-21, 2008, Dallas, TX., USA.
- Storm, M., 2009. Fast-electron source characterization and transport in high-intensity laser-solid interactions and the role of resistive magnetic fields. Doctoral Thesis, Institute of Optics, University of Rochester, New York, USA.